Structural Properties of Apocytochrome b_5: Presence of a Stable Native Core†

Cathy D. Moore and Juliette T. J. Lecomte*

Department of Chemistry, The Pennsylvania State University, University Park, Pennsylvania 16802

Received November 15, 1989; Revised Manuscript Received December 18, 1989

ABSTRACT: Upon removal of the heme group, the water-soluble fragment of cytochrome b_5 adopts a conformation less stable and compact than that of the holoprotein [Huntley, T. E., & Strittmatter, P. (1972) *J. Biol. Chem. 247*, 4641–4647]. This conformation, imposed by the amino acid sequence alone, has not been described in detail. One- and two-dimensional proton nuclear magnetic resonance spectroscopy techniques were applied to the apoprotein of the soluble fragment of rat liver cytochrome b_5 in an effort to characterize the structure of the apoprotein. Nuclear Overhauser spectroscopy revealed a number of short interresidue distances and demonstrated that, in spite of the increased flexibility, at least one cluster of side chains exists on a time scale long enough for study. Several residues participating in the cluster, in particular the only Trp (Trp 22), were identified. Similarities with the spectrum of the reduced holoprotein were observed that led to the inspection of the cytochrome b_5 crystal structure for assigning resonances. It appeared that the environment of this residue maintains its integrity in the apoprotein. Since in the holoprotein Trp 22 belongs to a hydrophobic core formed in part by β-strands, it is proposed that some of this β-structure is stable in the absence of the heme–protein interactions. Implications for structure and folding are discussed.

The structural and thermodynamic properties of *b* heme proteins depend strongly on the presence of the prosthetic group. Myoglobin and hemoglobin are well-known examples that exhibit severe losses of stability and secondary structure when the heme is extracted (Harrison & Blout, 1965; Breslow et al., 1965; Yip et al., 1972). The characteristics of the structure remaining in apo *b* heme proteins have not been investigated in detail. Yet, a high-resolution description of the conformation they adopt in solution would help to define the contribution of the heme to the native fold and reveal the information encoded in the sequence. It would also provide insight into the unique affinity for the heme and the mechanism of its insertion. We report here results obtained on the apoprotein of the water-soluble fragment of cytochrome b_5.

Hepatic cytochrome b_5 is a monomeric heme protein participating in electron-transport reactions (Mathews & Czerwinski, 1976). The protein contains two independent domains: a heme-containing hydrophilic region, referred to as cyt b_5[1] hereafter, and a hydrophobic tail anchoring the protein to the endoplasmic reticulum (Spatz & Strittmatter, 1971; Visser et al., 1975). The crystal structure of oxidized ovine liver cyt b_5 has been solved (Mathews et al., 1971). It has a globular shape formed by six helices, five strands arranged in a pleated sheet, and several β-turns. The heme, bound to the protein by coordination to two histidines (His 39 and 63), resides in a crevice formed by four of the helices. The residues lining the cavity are mostly nonpolar and constitute a hydrophobic core (core 1); a second hydrophobic core (core 2) is located on the other side of the molecule, more than 15 Å away from the iron. The role of this second core is unclear. Numerous spectroscopic techniques, including NMR (Keller et al., 1976; Keller & Wüthrich, 1980; Reid et al., 1987; Rodgers et al., 1988; McLachlan et al., 1988; Veitch et al., 1988; Altman et al., 1989; T. C. Pochapsky, S. G. Sligar, S. J. McLachlan and G. N. La Mar, personal communication), have been applied to cyt b_5 in order to investigate its functional and structural properties. The holoprotein is therefore well described.

Upon heme extraction, cyt b_5 undergoes conformational changes that result in a much-altered heme-free protein (apocyt b_5). Hydrodynamic measurements (Huntley & Strittmatter, 1972), as well as susceptibility to chemical denaturants (Tajima et al., 1976) and proteolysis (Strittmatter & Ozols, 1966), indicate that apocyt b_5 is less compact and less stable than the holoprotein while CD spectra suggest an increase in disorder and a redistribution of secondary elements (Huntley & Strittmatter, 1972). Our approach to the study of apocyt b_5 is to apply one- and two-dimensional proton NMR techniques. We show here that it is indeed possible to describe precisely some of the structural features of the apoprotein. We provide evidence that apocyt b_5 is not fully unfolded under normal conditions of pH and temperature and that at least one extended region of the apoprotein, overlapping with the second hydrophobic core, can be compared directly to the native holoprotein.

Experimental Procedures

Protein Preparation. Rat liver cyt b_5 is the protein used in this work. It is highly homologous to the beef liver protein (Ozols & Heinemann, 1982).[2] The soluble fragment, expressed from a synthetic gene in *Escherichia coli*, was prepared

†Supported in part by BRSG Grant S07 RR07082-22 awarded by the Biomedical Research Support Grant Program of the National Institutes of Health and in part by Grant GM 33775 from the National Institutes of Health to the laboratory of Dr. S. G. Sligar.

* To whom correspondence should be addressed.

[1] Abbreviations: apocyt b_5, apo form of the water-soluble fragment of cytochrome b_5; CD, circular dichroic; COSY, two-dimensional correlated spectroscopy; cyt b_5 or holocyt b_5, water-soluble fragment of cytochrome b_5; DQF-COSY, double-quantum-filtered COSY; NMR, nuclear magnetic resonance; NOE, nuclear Overhauser effect; NOESY, two-dimensional nuclear Overhauser spectroscopy; SDS–PAGE, sodium dodecyl sulfate–polyacrylamide gel electrophoresis.

[2] Rat liver cyt b_5 is composed of 98 residues, 5 more than the calf liver protein. In the common 93-residue segment, there are 12 replacements, only one of which (Tyr27His) is truly nonconservative. In this work, the residues are numbered according to the calf liver scheme, i.e., from residue −4 to residue 94.

0006-2960/90/0429-1984$02.50/0

from crude cell extracts generously provided by Dr. S. G. Sligar (University of Illinois at Urbana–Champaign). The reported method of purification was followed (Beck von Bodman et al., 1986) and resulted in a single band by SDS–PAGE and an absorbance ratio A_{412}/A_{280} of 5.8–6.3. The apoprotein was obtained from the freshly purified material according to the methyl ethyl ketone procedure of Teale (1959). Recovery of the apoprotein was better than 80%. Residual holoprotein accounts for less than 5% of the total protein as evaluated from the A_{412}/A_{280} value; the corresponding proton signals were not detected in the apoprotein NMR spectrum.

NMR Samples. Sample concentrations were typically 0.75–1.5 mM for one-dimensional and 1.7–2.5 mM for two-dimensional NMR experiments. Sample pH was adjusted with a Beckman Phi71 pH meter equipped with an Ingold combination microelectrode. ^2H_2O samples were exchanged and lyophilized two to three times before use. The pH of these samples (pH*) was not corrected for isotope effect.

NMR Experiments. ^1H NMR spectra were recorded on a Bruker AM-500 spectrometer operating in the quadrature mode at a proton frequency of 500 MHz. The probe temperature was maintained at 298 K. DQF-COSY (Rance et al., 1983) and phase-sensitive NOESY spectra (Kumar et al., 1980) were acquired according to the standard procedure. Quadrature detection in the ω_1 dimension was implemented through the time proportional increment method (Drobny et al., 1979; Marion & Wüthrich, 1983). The carrier and decoupler frequencies were placed on the $^1H^2HO$ line in all two-dimensional experiments; transmitter and decoupler were phase-coherent. The 90° transmitter pulse was of the order of 7 μs, and the sweep width was 7042 Hz in both dimensions. Typically, a matrix of 2048 complex points (t_2) × 512 (t_1) data points was acquired; 64 (DQF-COSY) or 128 (NOESY) transients were added for each t_1 value. Water elimination was achieved with presaturation of the resonance with a 1-s decoupler pulse. NOESY spectra were recorded with mixing times ranging from 100 to 200 ms. No evidence of spin diffusion was found. Data processing was performed with the FTNMR program of Dr. D. Hare (Hare Research Inc.) on a DEC Microvax II. The raw data matrix was transformed with zero filling in the t_1 dimension to obtain a 2048 × 1024 complex-point matrix. A polynomial base-line correction (third order) was applied to the ω_2 domain before transforming in the t_1 domain. Data were filtered in both dimensions with phase-shifted sine-bell window functions. For the NOESY data, the free induction decay corresponding to the first t_1 value was divided by 2 to suppress ridges in the ω_1 dimension (Otting et al., 1986). All spectra were processed and plotted in the phase-sensitive mode. Chemical shifts are referred to the $^1H^2HO$ line at 4.76 ppm.

Results

Figure 1 presents the 500-MHz ^1H NMR spectrum of apocyt b_5 at pH 6.2, 298 K, in ^2H_2O. The resolved resonances in the aromatic and high-field aliphatic regions are typical of a polypeptide possessing some degree of nonstatistical structure (Bundi & Wüthrich, 1979; Wüthrich, 1986). For example, signals between 4.8 and 6.2 ppm are indicative of C^α protons located within β-structure (Dalgarno et al., 1983), and the signal at ca. −1 ppm (a) arises from a methyl group subjected to a strong ring-current shift. The environment of this group was probed by one-dimensional nuclear Overhauser spectroscopy (Noggle & Schirmer, 1971). Saturation of the line perturbs the intensity of several signals in the aliphatic and aromatic regions. This exploratory experiment demonstrated

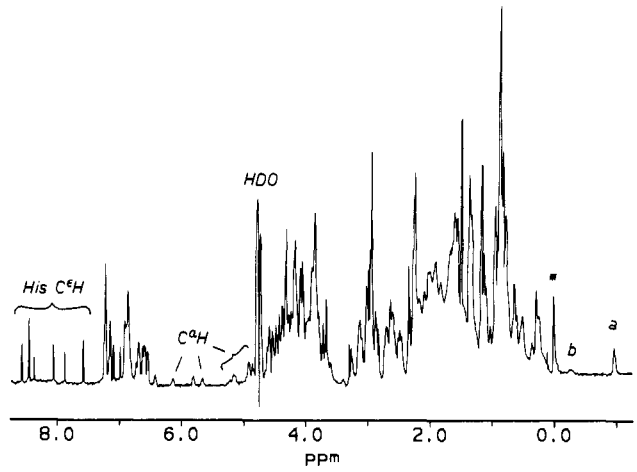

FIGURE 1: 500-MHz proton spectrum of apocyt b_5 in ^2H_2O at pH* 6.20, 298 K. The chemical shift dispersion is indicative of a folded structure. Clearly resolved are the histidine C^ϵ protons and several C^α protons. The peaks labeled a and b are ring-current-shifted methyl group and single proton, respectively. The (*) denotes an impurity.

that apocyt b_5 possesses at least one stable cluster of aromatic and aliphatic residues and that further NMR characterization was feasible.

The assignment of the residues forming the cluster was achieved by two-dimensional spectroscopy in ^2H_2O at pH* 7.1 and 298 K. Figure 2 presents selected sections of the phase-sensitive NOESY map which display dipolar connectivities to aromatic side chains. It illustrates two features of the apocyt b_5 spectrum: the lines are well resolved, and a large number of strong interresidue contacts are detected. Rat liver apocyt b_5 contains four Tyr residues (Tyr 6, 7, 30, and 74), two Phe residues (Phe 35 and 58), one Trp residue (Trp 22), and six His residues (His 15, 26, 27, 39, 63, and 80). All the aromatic protons are identifiable with DQF-COSY and NOESY experiments. Of particular usefulness to this work is the sole Trp residue. In the DQF-COSY spectrum (not shown) Trp 22 exhibits a resolved pattern of two triplets ($C^{\zeta_3}H$ and $C^{\eta_2}H$) and two doublets ($C^{\zeta_2}H$ and $C^{\epsilon_3}H$). In the NOESY map the expected intraresidue effects are marked 2, 3, 6, and 9. Cross peaks 1, 4, 5, 7, 8, 10, 11, and 12 are all manifestations of interaromatic dipolar contacts. Precise topological information can be obtained from the latter connectivities provided that the $C^{\zeta_3}H$ and $C^{\eta_2}H$ triplets and the $C^{\zeta_2}H$ and $C^{\epsilon_3}H$ doublets are distinguished. An NOE experiment in ^1H_2O resolves the issue (Figure 2C). In ^1H_2O, the exchangeable ring $N^\epsilon H$ of Trp residues is present and yields strong NOES to the $C^{\zeta_2}H$ and the $C^\delta H$ resonances of the same residue. One apocyt b_5 exchangeable proton signal, at 9.33 ppm, has NOEs to a nonidentified singlet at 6.93 ppm (cross peak 14) and a Trp 22 doublet at 6.69 ppm (cross peak 13). This assigns the doublet to the $C^{\zeta_2}H$ and the singlet to the $C^\delta H$ of Trp 22. The latter proton is in dipolar contact with a C^α proton at 6.14 ppm (cross peak 15), consequently attributed to the same side chain. The chemical shift values for Trp 22 ring protons in apocyt b_5 (listed in Table I) are clearly distinct from those in the statistical coil but differ by at most 0.13 ppm from those of the reduced (ferro, diamagnetic) cyt b_5 (T. C. Pochapsky, S. G. Sligar, S. J. McLachlan, and G. N. La Mar, personal communication) and by at most 0.20 ppm from those of the oxidized (ferric, paramagnetic) cyt b_5 (Reid et al., 1987). This points to similar environments around position 22 in the three forms of the protein.

By referring to DQF-COSY results, interresidue cross peaks 4 and 7 are traced to a His residue. Cross peaks 1, 5, 8, and

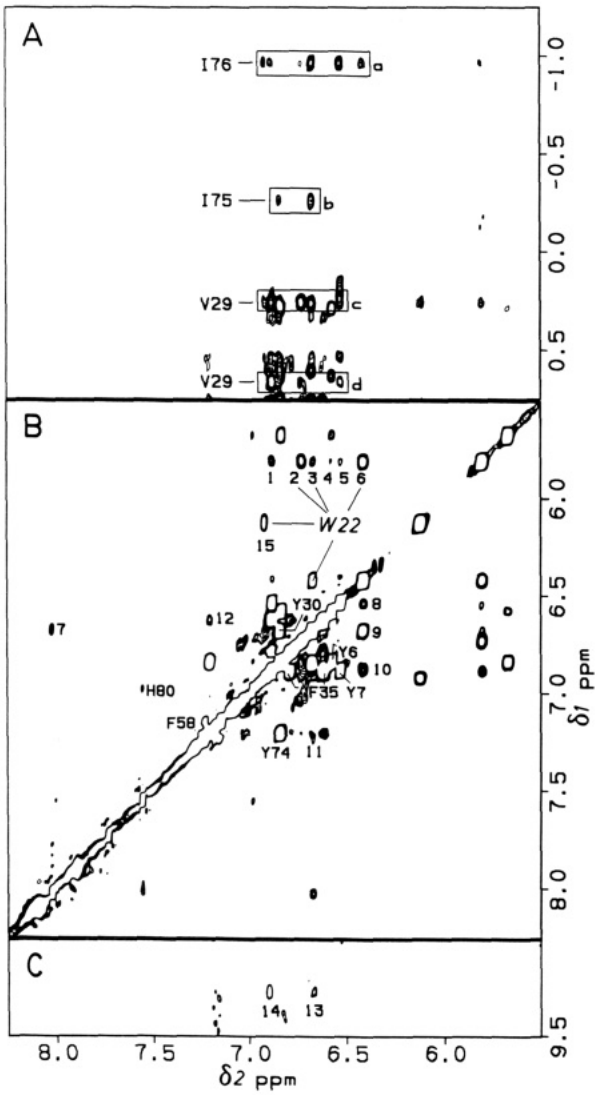

FIGURE 2: NOESY spectrum of a 2.1 mM sample of apocyt b_5 at 298 K recorded with a mixing time of 100 ms; connectivities involving the aromatic side chains. (A) Upfield-shifted aliphatic/aromatic connectivities in ^2H_2O, pH* 7.1. Box a contains the NOEs to the $C^\delta H_3$ of Ile 76; box b contains the NOEs to a $C^\gamma H$ of Ile 75; boxes c and d contain, among others, the NOEs to the two $C^\gamma H_3$ groups of Val 29. (B) Aromatic/aromatic connectivities; conditions the same as for (A). Cross peaks marked 2, 3, 6, 9, and 15 arise from intraresidue contacts in Trp 22. Other intraresidue cross peaks are labeled directly according to the assignments. Cross peaks marked 1, 4, 5, 7, 8, 10, 11, and 12 are interresidue contacts. (D) Aromatic/NH connectivities in 90% ^1H_2O/10% ^2H_2O, pH 5.75. Cross peaks 13 and 14 arise from Trp 22. See text for a discussion of the assignments.

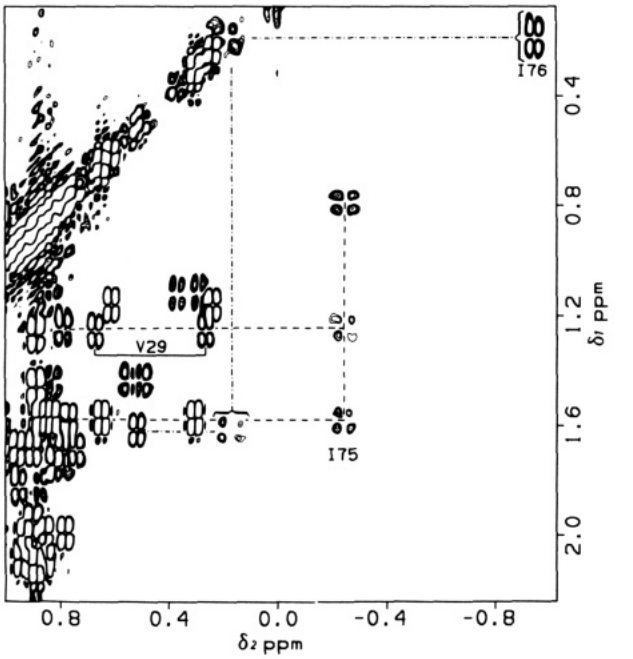

FIGURE 3: Portion of a 500-MHz DQF-COSY spectrum of a 1.7 mM sample of apocyt b_5 in ^2H_2O at 298 K, pH* 6.15. Positive and negative contours are plotted without distinction. The region contains $C^\beta H$–$C^\gamma H_3$ and $C^\beta H$–$C^{\gamma\prime} H_3$ cross peaks of valine residues, $C^\gamma H$–$C^\delta H_3$ and $C^\gamma H$-$C^{\delta\prime} H_3$ cross peaks of leucine residues, and $C^\beta H$–$C^\gamma H_3$, $C^\gamma H$–$C^\delta H_3$, and $C^\gamma H'$–$C^\delta H_3$ cross peaks of isoleucine residues. Three relevant sets are marked: (–·–) Ile 76 with degenerate C^γ geminal protons, (––) Ile 75 with one upfield-shifted $C^\gamma H$ (peak b in Figure 1), and (—) Val 29.

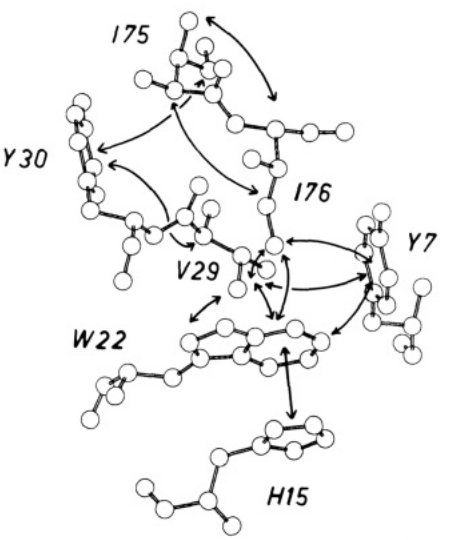

FIGURE 4: Part of the environment of Trp 22 in the beef holoprotein, according to the X-ray structure (Mathews & Czerwinski, 1971). The interresidue NOE connectivities observed in the apoprotein spectrum are marked by arrows.

10 arise from contact with a Tyr residue. The NOEs connecting upfield-shifted protons to the aromatic residues are shown in Figure 2A. The cross peaks in box a correspond to the effects observed in the one-dimensional experiment: the methyl group at ca. −1 ppm is in dipolar contact with Trp 22 and the Tyr ring. A pair of methyl groups close to both aromatic rings is found at 0.67 and 0.27 ppm (Figure 2A, cross peaks in boxes c and d). Even at a longer mixing time of 200 ms, the tyrosine ring and these methyl groups do not yield NOEs to the histidine residue.

The DQF-COSY spectrum was used to identify the aliphatic residues packed against Trp 22. A representative portion of the spectrum is shown in Figure 3. The resonance at ca. −1 ppm is a triplet attributed to the $C^\delta H_3$ of an Ile residue. The two methyl signals at 0.67 and 0.27 ppm are doublets belonging to the same Val side chain. Thus, in the apoprotein Trp 22 is surrounded by a Tyr, a His, a Val, and an Ile residue. To obtain sequence-specific information on these side chains, the X-ray structure of the holoprotein is consulted. Such procedure is prompted by the nearly unchanged chemical shifts of Trp 22 and by fluorescence and CD data indicating that the environment of this residue remains native-like in the apoprotein (Huntley & Strittmatter, 1972). The holoprotein environment of Trp 22 includes Tyr 7, His 15, Val 29, and Ile 76, oriented as illustrated in Figure 4.[3] Also in this figure

[3] F. S. Mathews and E. W. Czerwinski; coordinates deposited in the Brookhaven Protein Data Bank (2b5c).

Table I: ^{1}H Chemical Shifts (ppm) of Apo-, Ferro-, and Ferricyt b_5

residue	proton[a]	apo[b]	ferro[c]	ferri[d]	random coil[e]
Trp 22	$C^{\alpha}H$	6.14	6.51[f]	6.16[f]	4.70
	$C^{\delta}H$	6.93			7.24
	$N^{\epsilon}H$	9.33			10.22
	$C^{\eta}H$	6.74	6.79	6.55	7.65
	$C^{\zeta}H$	5.81	5.94	5.69	7.17
	$C^{\gamma}H$	6.43	6.52	6.33	7.24
	$C^{\zeta}H$	6.69	6.78	6.65	7.50
Tyr 6	$C^{\delta}H$	6.84	6.91	6.81	7.15
	$C^{\epsilon}H$	6.59	6.65	6.53	6.86
Tyr 7	$C^{\delta}H$	6.88	6.98	6.87	7.15
	$C^{\epsilon}H$	6.53	6.63	6.51	6.86
His 15	$C^{\epsilon}H$	8.03	7.98	7.89	8.12
	$C^{\delta}H$	6.59	6.88	6.86	7.14
Val 29	$C^{\alpha}H$	4.52	4.46[b]		4.18
	$C^{\beta}H$	1.26	1.20[b]		2.13
	$C^{\gamma}H_3$	0.67, 0.27	0.74,[b] 0.25[b]		0.97, 0.94
Tyr 30	$C^{\delta}H$	6.84	7.21	6.57	7.15
	$C^{\epsilon}H$	6.69	6.92	6.42	6.86
Phe 35	$C^{\delta}H$	6.63/6.91	6.52		7.30
	$C^{\epsilon}H$	6.91/6.63	6.22		7.39
	$C^{\zeta}H$	6.80	6.97		7.34
Phe 58	$C^{\delta}H$	7.15			7.30
	$C^{\epsilon}H$	7.24	5.20		7.39
	$C^{\zeta}H$		5.53		7.34
Tyr 74	$C^{\delta}H$	6.85/7.20	7.21	7.14	7.15
	$C^{\epsilon}H$	7.20/6.85	6.46	6.76	6.86
	$C^{\zeta}H$[g]			7.01	
Ile 75	$C^{\alpha}H$	3.81			4.23
	$C^{\beta}H$	1.58			1.90
	$C^{\gamma}H$	−0.25, 1.25			1.48, 1.19
	$C^{\gamma}H_3$	0.77			0.95
	$C^{\delta}H_3$	0.79			0.89
Ile 76	$C^{\alpha}H$	4.40			4.23
	$C^{\beta}H$	1.62			1.90
	$C^{\gamma}H$	0.19, 0.19	0.18, 0.42	0.16, −0.10	1.48, 1.19
	$C^{\gamma}H_3$	0.53			0.95
	$C^{\delta}H_3$	−0.96	−0.93	−1.17	0.89
His 80	$C^{\epsilon}H$	7.56		7.52	8.12
	$C^{\delta}H$	7.00		6.95	7.14

[a] We use the rules of the IUPAB–IUB Commission on Biochemical Nomenclature (1970). [b] Chemical shift of nonexchangeable protons determined at pH* 7.1 and 298 K; chemical shift of exchangeable protons determined at pH 5.8 and 298 K. [c] From T. C. Pochapsky, S. G. Sligar, S. J. McLachlan, and G. N. La Mar, personal communication; determined at pH* 6.8, 298 K, in the presence of 50 mM phosphate buffer. The most populated isomer is used except for Ile 76. [d] From Reid et al. (1987); determined at pH* 7.0, 297 K, in the presence of 50 mM phosphate buffer. Chemical shifts for ferricyt b_5 are reported for the beef protein. [e] From Bundi and Wüthrich (1979). [f] From Veitch et al. (1988); determined at pH 7.0, 303 K, in the presence of 20 mM phosphate buffer on the beef protein. [g] Position 74 is occupied by Phe in the beef protein.

is a summary of the interresidue NOEs detected in the apoprotein cluster. The overall consistency of the match allows us to assign tentatively those four side chains.

Other interresidue NOEs are observed. Cross peaks 11 and 12 in Figure 2B arise from a Tyr in contact with a Phe and another Tyr. The X-ray structure of the beef protein offers only one set of three aromatic residues properly positioned: Tyr 30, Phe 35, and Phe 74. However, in the rat liver protein Phe 74 is replaced by a Tyr.[4] Thus, the NOE cross peaks in the rat apoprotein are likely to arise from Tyr 74, Phe 35, and Tyr 30. Tyr 30 is tentatively distinguished from Tyr 74 by a weak NOE to the $C^{\alpha}H$ of Val 29. As shown in Figure 2A (cross peaks in box b), Tyr 30 has NOEs to one of the C^{γ} geminal protons of the second Ile spin system traced in Figure 3. In addition, NOEs from the $C^{\alpha}H$ of this Ile to the degenerate $C^{\gamma}H_2$ of Ile 76 and from its $C^{\gamma}H_3$ to the $C^{\alpha}H$ of Ile 76 consolidate the assignment to Ile 75 (Figure 4). The second Phe in the spectrum is assigned by process of elimination to Phe 58. Phe 58, normally buried in the heme pocket, has few NOEs in the apoprotein. As for the remaining Tyr, Tyr 6, its $C^{\epsilon}H$'s and $C^{\delta}H$'s show NOEs to the $C^{\delta}H$ of a His residue at 7.00 ppm when the mixing time is extended to 200 ms. On the basis of the crystal structure and reported chemical shift values (Reid et al., 1987; Altman et al., 1989), this histidine is assigned to His 80.

[4] Tyr 74 is a Phe in the crystal structure. The same orientation of the ring is assumed.

Discussion

Cyt b_5 contains only one Trp residue, Trp 22, which provides a reliable starting point for the assignment process. To analyze the apoprotein spectrum, we inspected the environment of this side chain in the X-ray structure of oxidized beef liver cyt b_5. NMR studies on beef liver cyt b_5 (Keller et al., 1976; Keller & Wüthrich, 1980; Reid et al., 1987; Veitch et al., 1988; McLachlan et al., 1988) and rat liver cyt b_5 (T. C. Pochapsky, personal communication) have not revealed any major discrepancies with the corrected solid-state structure (Mathews, 1980). Thus, the holoprotein of rat cyt b_5 in solution is, to a first approximation, adequately represented by the beef model. In the holoprotein, Tyr 7, His 15, Val 29, and Ile 76 participate in the direct surroundings of the tryptophan ring. These residues are far from the heme pocket and practically not under the influence of the iron–protoporphyrin ring current. In the apoprotein, the same amino acid composition (i.e., Tyr, His, Val, Ile) is identified, and the chemical shifts of the corresponding resonances are similar. Constructing around Trp 22 a native-like core formed by residues different from the holoprotein (i.e., not 7, 15, 29, 76) appears unlikely. The

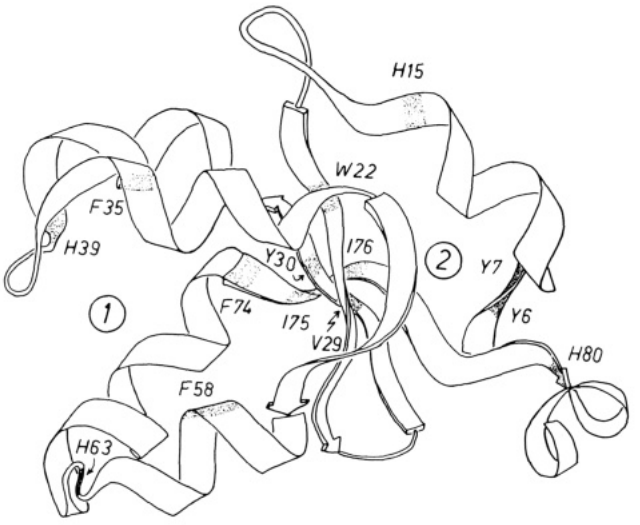

FIGURE 5: Ribbon diagram of beef liver holocyt b_5. The circled numbers 1 and 2 indicate the approximate location of hydrophobic cores 1 and 2, respectively. The heme, removed for clarity, fits in hydrophobic core 1 defined by the four helices on the left of the structure. The C^{α} of the residues of interest to this work are marked on the ribbon by a shaded area. The two histidine side chains coordinated to the heme are H39 and H63. In the rat protein, F74 is replaced by Y74.

-Ile-Ile- connectivities eliminate the possibility of a cluster involving an Ile residue sequentially closer to Trp than Ile 76 since there is only one such doublet in the sequence. The same argument applies to Val 29 as indicated by the NOE to Tyr 30.

Structural agreement between holo- and apoprotein is expected to break down in many locations, and referring to the X-ray model for assignment purposes will not be generally warranted. However, the formation of a stable cluster imposes severe restrictions on the conformational space accessible to the rest of the polypeptide chain. For instance, the NOEs between Tyr 74 and Tyr 30 and those to Phe 35 are consistent with the constraints imposed by Ile 76 and spatially nearby Val 29 on the rest of the structure. Also dependent on the cluster are Tyr 6 and His 80, which form similar contacts in the apo- and holoprotein (see below).

Another test of the structural resemblance, more reliable and stringent than chemical shift values, is the comparison of the NOEs presented here to those detected in the holoprotein. This additional verification accounts for possible deviations between the X-ray structure of beef liver cyt b_5 and the solution structure of rat liver cyt b_5. We have recorded a NOESY spectrum of the reduced holoprotein under the conditions used for apocyt b_5. Examination of two-dimensional maps of the holoprotein [not shown, see Rodgers et al. (1988)] confirmed the following networks of NOE connectivities: His 15 ↔ Trp 22, Trp 22 ↔ Tyr 7, Trp 22 ↔ Ile 76, Val 29 ↔ Trp 22, Tyr 7 ↔ Ile 76, Val 29 ↔ Tyr 7, Val 29 ↔ Ile 76, and Tyr 6 ↔ His 80. The NOEs corresponding to the Phe 35 ↔ Tyr 74 ↔ Tyr 30 group are not observed in the rat holoprotein. This may be due to the heme rotational isomers, which are present in approximately equal proportions. The resonances of these three residues are well resolved in the two forms, and this results in a weakening of the expected NOEs. Furthermore, Phe 35 is in the heme pocket, and both isomers exhibit broad lines. NOEs between Phe 74 and Tyr 30 do appear in the beef holoprotein where the isomer ratio is 9:1 (Reid et al., 1987).

Figure 5 illustrates that the identified side chains are found in different regions of the holoprotein. The residues within the β-sheet, Tyr 6, Tyr 7, Tyr 74, Ile 75, Ile 76, Val 29, Tyr 30, and Trp 22, sample four of the five strands forming the back wall of the heme pocket. When the heme is removed, they remain in the holoprotein orientation, poised as expected from the formation of the secondary structure. The connectivities between Tyr 6 and His 80 indicate the proper docking of the two ends of the molecule. Tyr 30 and Tyr 74 are in the β-sheet and are directed toward the heme crevice. Phe 35, on the other hand, is located in the center of the helix ending with His 39. Its NOEs to Tyr 74 suggest that it is in the native position. In contrast, Phe 58, the only residue assigned so far in the helix leading to His 63, appears exposed to the solvent.

Our observations indicate the formation of a compact region of the structure stabilized by hydrophobic interactions. Specific compact states with a high degree of secondary structure have been referred to as "molten globules" (Ptitsyn, 1987) or "A states". The A state has a fluctuating tertiary structure which is responsible for NMR spectra resembling those of the unfolded state (Baum et al., 1989). Apocyt b_5 displays a number of long-lived tertiary interactions even at pH 5.8. This information argues against the apoprotein being fully in one of those states under our experimental conditions. It is interesting that Trp 22 is largely protected against solvent exposure in the holoprotein (only the C^{ζ_2} and C^{η_2} protons are partly accessible) and remains so in the apoprotein. This is a strong indication of the structural importance of a stable core (Tanford, 1980) and may provide an explanation for the rigorous conservation of the constitutive residues across the cytochrome b_5 family (Mathews et al., 1979).

Apocytochrome b_5 is synthesized on the endoplasmic reticulum (Gonzalez & Kasper, 1908; Krieter & Shires, 1980); insertion of the iron in the porphyrin takes place in the mitochondrion (Jones & Jones, 1969). How and when the heme meets the polypeptide have not been established. Radioactive labeling experiments (Negishi & Omura, 1970; Hara & Minikami, 1970; Hara et al., 1970) and immunological assays (Shawver et al., 1984) indicate that a pool of excess apocytochrome b_5 exists in the microsomes. In vitro experiments designed to determine the mechanism of heme transport through the cytoplasm have shown a transfer rate on the order of tens of seconds when accelerated by the enzyme glutathione *S*-transferase (Senjo et al., 1985). Thus, apocytochrome b_5 may be required to maintain a stable conformation during a lag phase prior to heme insertion. The presence of β-sheet structure or a specific hydrophobic core dictated by the primary sequence alone could direct the formation of a rudimentary heme pocket, position the ligand His residues so as to increase the affinity for the heme, and facilitate completion of the folding process. Further studies on the hydrogen-bond network, the complete hydrophobic core 2 and the details of its geometry, and the state of the His residues are in progress.

ACKNOWLEDGMENTS

Some of the protein used in this study was expertly prepared by Dr. T. C. Pochapsky and kindly given to us by Dr. S. G. Sligar. Purification of cell extracts was guided by advice from Mark Chiu and Susan Martinez. The first one-dimensional experiments were performed at the University of California at Davis through the generosity of Dr. G. N. La Mar. Numerous discussions with Dr. T. C. Pochapsky and Dr. C. R. Matthews and their critical reading of the manuscript were most helpful.

REFERENCES

Altman, J., Lipka, J. J., Kuntz, I., & Waskell, L. (1989) *Biochemistry 28*, 7516–7523.

Anfinsen, C. B. (1973) *Science 181*, 223–230.
Baum, J., Dobson, C. M., Evans, P. A., & Hanley, C. (1989) *Biochemistry 28*, 7–13.
Beck von Bodman, A., Schuler, M. A., Jollie, D. R., & Sligar, S. G. (1986) *Proc. Natl. Acad. Sci. U.S.A. 83*, 9443–9447.
Breslow, E., Beychok, S., Hardman, K. D., & Gurd, F. R. N. (1965) *J. Biol. Chem. 240*, 304–309.
Bundi, A., & Wüthrich, K. (1979) *Biopolymers 18*, 285–297.
Dalgarno, D. C., Levine, B. A., & Williams, R. J. P. (1983) *Biosci. Rep. 3*, 443–452.
Drobny, G., Pines, A., Sinton, S., Weitekamp, D. P., & Wemmer, D. (1979) *Symp. Faraday Soc. 13*, 49–55.
Gonzalez, F. J., & Kasper, C. B. (1980) *Biochemistry 19*, 1790–1769.
Hara, T., & Minakami, S. (1970) *J. Biochem. 67*, 741–744.
Hara, T., Tanaka, S., & Minakami, S. (1970) *J. Biochem. 68*, 805–810.
Harrison, S. C., & Blout, E. R. (1965) *J. Biol. Chem. 240*, 299–303.
Huntley, T. E., & Strittmatter, P. (1972) *J. Biol. Chem. 247*, 4641–4647.
IUPAC–IUB Commission on Biochemical Nomenclature (1970) *Biochemistry 9*, 3471–3479.
Jones, M., & Jones, O. (1969) *Biochem. J. 113*, 507–514.
Keller, R. M., & Wüthrich, K. (1980) *Biochim. Biophys. Acta 621*, 204–217.
Keller, R. M., Groudinsky, O., & Wüthrich, K. (1976) *Biochim. Biophys. Acta 427*, 497–511.
Krieter, P. A., & Shires, T. K. (1980) *Biochem. Biophys. Res. Commun. 94*, 606–611.
Kumar, A., Ernst. R. R., & Wüthrich, K. (1980) *Biochem. Biophys. Res. Commun. 95*, 1–6.
Marion, D., & Wüthrich, K. (1983) *Biochem. Biophys. Res. Commun. 113*, 967–974.
Mathews, F. S. (1980) *Biochim. Biophys. Acta 622*, 375–379.
Mathews, F. S., & Czerwinski, E. W. (1976) in *The Enzymes of Biological Membranes* (Martonosi, A., Ed.) Vol. 4, pp 143–197, Plenum Press, New York.
Mathews, F. S., Argos, P., & Levine, M. (1971) *Cold Spring Harbor Symp. Quant. Biol. 36*, 387–395.
Mathews, F. S., Czerwinski, E. W., & Argos, P. (1979) in *The Porphyrins* (Dolphin, D., Ed.) Vol. 7, pp 107–147, Academic Press, New York.
McLachlan, S. J., La Mar, G. N., Burns, P. D., Smith, K. M., & Langry, K. C. (1986) *Biochim. Biophys. Acta 874*, 274–284.
McLachlan, S. J., La Mar, G. N., & Lee, K.-B. (1988) *Biochim. Biophys. Acta 957*, 430–445.
Negishi, M., & Omura, T. (1970) *J. Biochem. 67*, 745–747.
Noggle, J. H., & Shirmer, R. E. (1971) in *The Nuclear Overhauser Effect*, Academic Press, New York.
Otting, G., Widmer, H., Wagner, G., & Wüthrich, K. (1986) *J. Magn. Reson. 66*, 187–193.
Ozols, J., & Heinemann, F. S. (1982) *Biochim. Biophys. Acta 704*, 163–173.
Ptitsyn, O. B. (1987) *J. Protein Chem. 6*, 273–293.
Rance, M., Sørensen, O. W., Bodenhausen, G., Wagner, G., Ernst, R. R., & Wüthrich, K. (1983) *Biochem. Biophys. Res. Commun. 117*, 479–485.
Reid, L. S., Gray, H. B., Dalvit, C., Wright, P. E., & Saltman, P. (1987) *Biochemistry 26*, 7102–7107.
Rodgers, K. K., Pochapsky, T. C., & Sligar, S. G. (1988) *Science 240*, 1657–1659.
Senjo, M., Ishibashi, T., & Imai, Y. (1985) *J. Biol. Chem. 260*, 9191–9196.
Shawver, L. K., Seidel, S. L., Krieter, P. A., & Shires, T. K. (1984) *Biochem. J. 217*, 623–632.
Spatz, L., & Strittmatter, P. (1971) *Proc. Natl. Acad. Sci. U.S.A. 68*, 1042–1046.
Strittmatter, P., & Ozols, J. (1966) *J. Biol. Chem. 241*, 4787–4792.
Tajima, S., Enomoto, K.-I., & Sato, R. (1976) *Arch. Biochem. Biophys. 172*, 90–97.
Tanford, C. (1980) *The Hydrophobic Effect*, Wiley, New York.
Teale, F. W. J. (1959) *Biochim. Biophys. Acta 35*, 543.
Veitch, N. C., Concar, D. W., Williams, R. J. P., & Whitford, D. (1988) *FEBS Lett. 238*, 49–55.
Visser, L., Robinson, N. C., & Tanford, C. (1975) *Biochemistry 14*, 1194–1199.
Wüthrich, K. (1986) in *NMR of Proteins and Nucleic Acids*, Wiley, New York.
Yip, Y. K., Waks, M., & Beychok, S. (1972) *J. Biol. Chem. 247*, 7237–7244.